



Oriented 2D Covalent Organic Framework Thin Films on Single-Layer Graphene

John W. Colson, et al. Science **332**, 228 (2011); DOI: 10.1126/science.1202747

This copy is for your personal, non-commercial use only.

If you wish to distribute this article to others, you can order high-quality copies for your colleagues, clients, or customers by clicking here.

Permission to republish or repurpose articles or portions of articles can be obtained by following the guidelines here.

The following resources related to this article are available online at www.sciencemag.org (this infomation is current as of April 8, 2011):

Updated information and services, including high-resolution figures, can be found in the online version of this article at:

http://www.sciencemag.org/content/332/6026/228.full.html

Supporting Online Material can be found at:

http://www.sciencemag.org/content/suppl/2011/04/05/332.6026.228.DC1.html

This article **cites 30 articles**, 5 of which can be accessed free: http://www.sciencemag.org/content/332/6026/228.full.html#ref-list-1

This article appears in the following **subject collections**: Chemistry

http://www.sciencemag.org/cgi/collection/chemistry

ethanol in the biomass conversion sector, to name but a few examples.

References and Notes

- 1. R. I. Masel, *Principles of Adsorption and Reaction on Solid Surfaces* (Wiley, Canada, 1996).
- 2. J. M. Thomas, W. J. Thomas, *Principles and Practice of Heterogeneous Catalysis* (VCH, Tokyo, 1996).
- 3. M. A. Barteau, Catal. Lett. 8, 175 (1991).
- J. K. Nørskov, M. Scheffler, H. Toulhoat, MRS Bull. 31, 669 (2006)
- G. A. Somorjai, Introduction of Surface Chemistry and Catalysis (Wiley, New York, 1994).
- B. C. Du, S. A. Rabb, C. Zangmeister, Y. Y. Tong, Phys. Chem. Chem. Phys. 11, 8231 (2009).
- F. T. Tan et al., Faraday Discuss. 140, 139, discussion 185 (2008).
- 8. C. P. Slichter, Annu. Rev. Phys. Chem. 37, 25 (1986).
- 9. T. M. Duncan, C. Dybowski, Surf. Sci. Rep. 1, 157 (1981).
- 10. J. J. van der Klink, H. B. Brom, *Prog. Nucl. Magn. Reson. Spectrosc.* **36**, 89 (2000).
- 11. Y. Y. Tong et al., J. Am. Chem. Soc. 124, 468 (2002).
- 12. R. D. Newmark, M. Fleischmann, B. S. Pons, J. Electroanal. Chem. 255, 325 (1988).

- 13. J. S. Bradley et al., Faraday Discuss. 92, 255 (1991).
- 14. K. Tedsree, A. T. S. Kong, S. C. Tsang, *Angew. Chem. Int. Ed.* **48**. 1443 (2009).
- 15. Materials and methods are detailed in supporting material on *Science* Online.
- 16. R. Van Hardeveld, F. Hartog, Surf. Sci. 15, 189 (1969).
- 17. Y. Y. Tong, A. Wieckowski, E. Oldfield, *J. Phys. Chem. B* **106**, 2434 (2002).
- 18.]. Wu et al., J. Chem. Soc., Faraday Trans. 93, 1017 (1997).
- A. Ruban, B. Hammer, P. Stoltze, H. L. Skriver,
 J. K. Norskov, J. Mol. Catal. Chem. 115, 421 (1997).
- R. Larsen, S. Ha, J. Zakzeski, R. I. Masel, J. Power Sources 157, 78 (2006).
- N. Aas, Y. X. Li, M. Bowker, J. Phys. Condens. Matter 3, 5281 (1991).
- 22. N. Akiya, P. E. Savage, AIChE J. 44, 405 (1998).
- H. F. Wang, Z. P. Liu, J. Phys. Chem. C 113, 17502 (2009).
- 24. M. D. Hughes et al., Nature 437, 1132 (2005).
- H. G. Fritsche, R. E. Benfield, Z. Phys. D At. Mol. Clust. 26 (suppl.), 15 (1993).
- 26. C. Rice et al., J. Power Sources 111, 83 (2002).
- 27. Y. X. Chen, M. Heinen, Z. Jusys, R. J. Behm, ChemPhysChem 8, 380 (2007).
- 28. J. X. Wang et al., J. Am. Chem. Soc. 131, 17298 (2009).

- 29. V. Stamenkovic *et al.*, *Angew. Chem. Int. Ed.* **45**, 2897
- 30. W. J. Zhou, J. Y. Lee, *Electrochem. Commun.* **9**, 1725
- 31. M. A. Rigsby *et al.*, *J. Phys. Chem. C* **112**, 15595 (2008).
- 32. The financial support of this work from the Engineering and Physical Sciences Research Council of the United Kingdom is acknowledged. The authors thank N. Rees, K. Yu, and A. Kong for technical assistance; K. Harrison of Oxford for providing simulated images; and B. Murrer and P. Collier of Johnson Matthey Technology Centre, UK, for helpful discussions. Support to the East China University of Science and Technology group from the 111 project is also acknowledged.

Supporting Online Material

www.sciencemag.org/cgi/content/full/332/6026/224/DC1 Materials and Methods

Figs. S1 to S13 Table S1 to S4 References

30 December 2010; accepted 1 March 2011 10.1126/science.1202364

Oriented 2D Covalent Organic Framework Thin Films on Single-Layer Graphene

John W. Colson, Arthur R. Woll, Arnab Mukherjee, Mark P. Levendorf, Eric L. Spitler, Virgil B. Shields, Michael G. Spencer, Jiwoong Park, William R. Dichtel R. Dichtel

Covalent organic frameworks (COFs), in which molecular building blocks form robust microporous networks, are usually synthesized as insoluble and unprocessable powders. We have grown two-dimensional (2D) COF films on single-layer graphene (SLG) under operationally simple solvothermal conditions. The layered films stack normal to the SLG surface and show improved crystallinity compared with COF powders. We used SLG surfaces supported on copper, silicon carbide, and transparent fused silica (SiO₂) substrates, enabling optical spectroscopy of COFs in transmission mode. Three chemically distinct COF films grown on SLG exhibit similar vertical alignment and long-range order, and two of these are of interest for organic electronic devices for which thin-film formation is a prerequisite for characterizing their optoelectronic properties.

ethods for crystallizing organic subunits into two-dimensional (2D) and three-dimensional (3D) covalent organic frameworks (COFs) remain in their infancy (1–4). COFs organize molecular components into periodic networks linked by covalent bonds, providing predictable structures with long-range order that is usually only found in noncovalent assemblies. These materials exhibit many desirable properties, including outstanding thermal stability, permanent porosity with high specific surface area, and the lowest densities of any organic material (5). However, the frameworks are inherently cross-linked and insoluble and are produced as either microcrystalline powders from solvothermal reactions or submonolayers by sublimation of the monomers onto crystalline metal surfaces (6–9). The limited utility of these forms precludes many applications for COFs. For example, 2D layered COFs incorporate functional π -electron systems into ordered structures ideally suited for optoelectronic devices (10–13). As unprocessable powders, these materials cannot be interfaced reliably to electrodes or incorporated into devices to harness or even quantify these properties. We now report the synthesis of oriented 2D layered COF films on single-layer graphene (SLG) surfaces.

The notable optical, electronic, and mechanical properties of SLG have attracted considerable interest, for example, as a possible replacement for tin-doped indium oxide transparent electrodes (14, 15). SLG's 2D, atomically precise structure is also well suited for interfacing to 2D layered networks. Large-scale graphene synthesis by metal-based chemical vapor deposition (CVD) has advanced dramatically in recent years (16–19), including

the high-throughput growth of 76-cm-wide samples supported on plastic substrates (20). We demonstrate that oriented COF films form under operationally simple solvothermal conditions on SLG supported by several different substrate materials: polycrystalline Cu films on Si wafers (SLG/Cu), fused SiO₂ (SLG/SiO₂), and SiC (SLG/SiC). The COF films are crystalline and oriented with their aromatic groups stacked perpendicular to the SLG surface on each substrate. Three boronate esterlinked COFs have been crystallized as thin films, including a square Ni phthalocyanine lattice of interest for organic photovoltaic devices (12, 13).

The solvothermal condensation of 1,4-phenylenebis(boronic acid) (PBBA) and 2,3,6,7,10,11hexahydroxytriphenylene (HHTP) in a mixture of mesitylene:dioxane (1:1 v/v) at 90°C in the presence of SLG/Cu forms a framework known as COF-5 (Fig. 1), as both an insoluble powder and as a continuous film on the graphene surface (21). Powder x-ray diffraction (PXRD) (fig. S1) and Fourier transform infrared spectroscopy of the unpurified powders (fig. S2) indicate that crystalline COF-5 is obtained with only minor amounts of residual reactants in as little as 1 hour (fig. S3), faster than the 72-hour reaction time used for its discovery (1). These observations prompted us to investigate whether graphene catalyzes COF-5 powder formation, but we obtained similar results in the absence of SLG (fig. S4). We conclude that long reaction times are not always necessary to produce COFs, suggesting that their films might be incorporated into devices more rapidly than previously thought.

We used synchrotron x-ray diffraction to compare the crystallinity of the COF-5 films and powders. Figure 2, A and B, shows 2D x-ray diffraction patterns obtained from a powder sample and a film grown on SLG/Cu, respectively, using identical incident beam and scan parameters. The data in Fig. 2A were collected in transmission mode by suspending a ~0.1-mm-thick powder sample perpendicular to the incident beam.

¹Department of Chemistry and Chemical Biology, Cornell University, Baker Laboratory, Ithaca, NY 14853, USA. ²Department of Electrical Engineering, Cornell University, Ithaca, NY 14853, USA. ³Cornell High Energy Synchrotron Source (CHESS), Ithaca, NY 14853, USA. ⁴Kavli Institute for Nanoscale Science, Cornell University, Ithaca, NY 14853, USA.

^{*}To whom correspondence should be addressed. E-mail: wdichtel@cornell.edu

The Bragg peaks in Fig. 2A appear as rings because of the random orientation of grains in the sample (see inset). For Fig. 2B, as well as all subsequent diffraction data obtained from films, we used grazing incidence diffraction (GID), in which the substrate surface is horizontal and nearly parallel to the incident beam. Axes labels Q_{\perp} and Q_{\parallel} (where $\hbar Q$ is the momentum transfer of a scattered photon, and \hbar is Planck's constant \hbar

divided by 2π) are defined using the convention $Q_{\perp} = 4\pi/\lambda \sin(\delta/2)$ and $Q_{\parallel} = 4\pi/\lambda \sin(v/2)$, where λ is the x-ray wavelength, and δ and v are the vertical and horizontal scattering angles, respectively (22). In contrast to Fig. 2A, the scattered intensity in Fig. 2B is concentrated near $Q_{\perp} = 0$, indicating that grains in the film exhibit fiber texture: Their c-axis orientations are centered on the surface normal, but they are randomly rotated about this axis

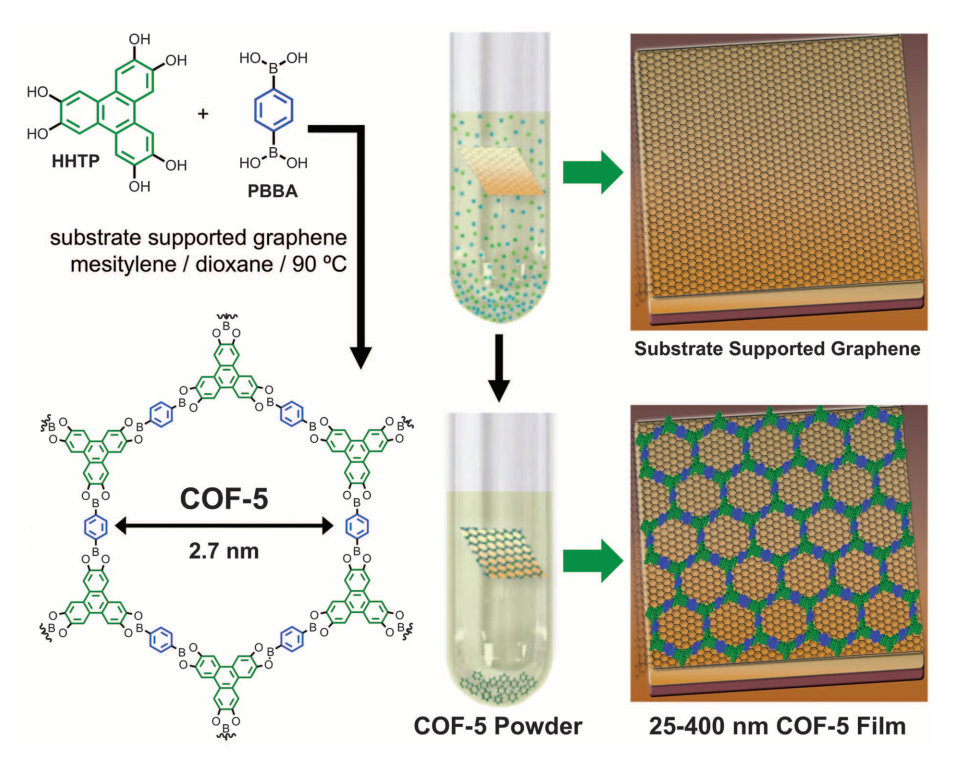


Fig. 1. Solvothermal condensation of HHTP and PBBA in the presence of a substrate-supported SLG surface provides COF-5 as both a film on the graphene surface, as well as a powder precipitated in the bottom of the reaction vessel.

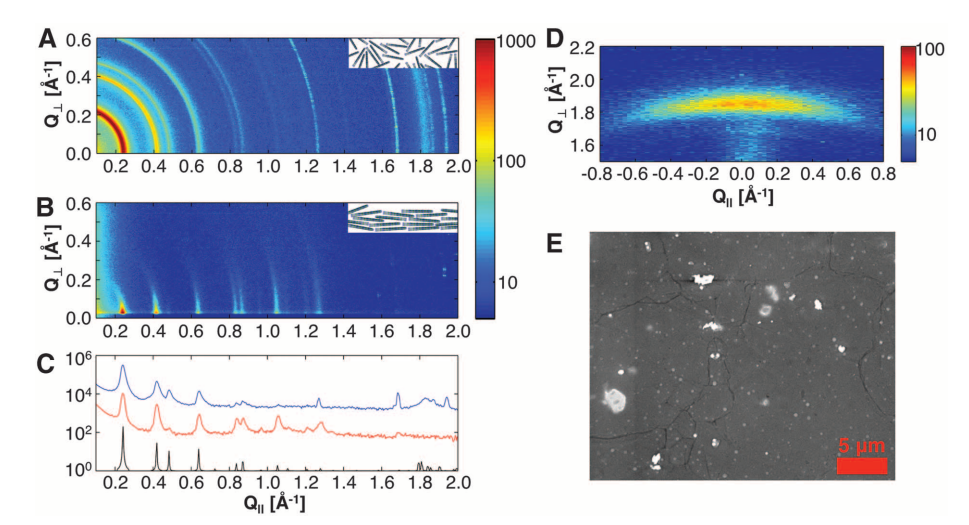


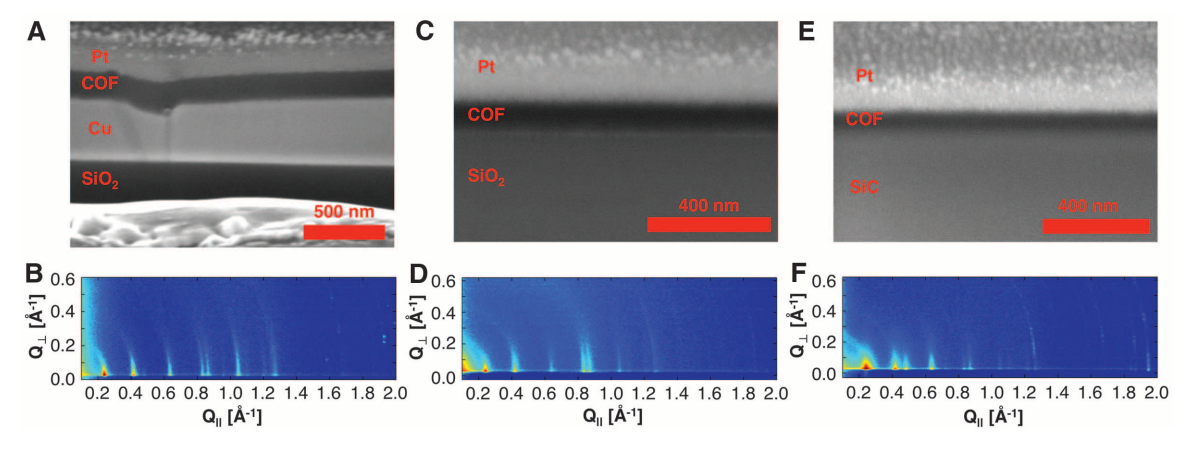
Fig. 2. (A) X-ray scattering data obtained from COF-5 powder; (inset) schematic of randomly oriented COF-5 grains in the powder, as indicated in (A). **(B)** GID data from a COF-5 film on SLG/Cu; (inset) schematic of oriented COF-5 grains in the film, as indicated in (B). **(C)** Projections of (A) (top/blue) and (B) (middle/red) near Q_{\perp} = 0, and the simulated powder diffraction spectrum (bottom/black) for COF-5. **(D)** GID data obtained at large Q_{\perp} , showing an off-specular projection of the COF-5 film (001) Bragg peak. **(E)** Top-down SEM image of the COF-5 thin film studied in (B), (C), and (D).

(see inset). Projections of these data sets near $Q_{\perp}=0$ (Fig. 2C) indicate peaks from both samples at 0.24, 0.42, 0.48, 0.64, 0.84, and 0.88 Å⁻¹, corresponding to 100, 110, 200, 210, 220, and 310 Bragg peaks of a hexagonal lattice with inplane lattice parameters a=b=29.9 Å, extremely close to the calculated (30.0 Å) and measured (29.7 Å) values previously reported for COF-5 powders (1). The concentration of these peaks near $Q_{\perp}=0$ in the film shows that the hexagonal lattice of the COF-5 grains is aligned parallel to the substrate surface.

Figure 2C highlights additional peaks not shared by both samples. First, the film exhibits diffraction peaks at 0.97, 1.06, 1.21, and 1.27 Å^{-1} that are not present in Fig. 2A or in reported PXRD of COF-5 powder. These peaks correspond to the COF-5 400, 320, 500, and overlapping 330 and 420 Bragg peaks. Additionally, the 200 peak (at 0.48 Å^{-1}) is attenuated in the film compared with the powder. This difference can arise from trace impurities in the pores or from subtle differences in the horizontal offset between layers in the film compared with the powder (23). Powder rings in Fig. 2A at 1.27, 1.68, 1.87, and 1.94 Å⁻¹ correspond to Bragg peaks from residual starting materials trapped in the pores of the unpurified powder samples. The broad powder ring in Fig. 2A centered at 1.83 Å⁻¹ corresponds to the 001 Bragg peak and indicates that the stacked COF-5 sheets are in van der Waals contact (with an out-of-plane lattice parameter c = 3.43 Å). This peak is absent in Fig. 2B because the c axes of grains in the film are oriented perpendicular to the substrate. Instead, the 001 peak of the film is observed (Fig. 2D) as a diffuse arc of scattering centered at $Q_{\perp} = 1.85 \text{ Å}^{-1}$ by obtaining additional measurements near $Q_{\parallel} = 0$ and a large out-of-plane diffraction angle, corresponding to large Q_{\perp} . The width of this peak in Q_{\parallel} provides a rough measure of the orientational order in the film (24) and indicates (see supporting online material text) that most grains orient their c axes within $\pm 13^{\circ}$ of the surface normal (fig. S5). Accounting for instrumental resolution and assuming platelet-shaped grains (25), Debye-Scherrer analysis of Fig. 2, B and D, indicates that the grains are $\sim 6.8 \pm 0.3$ nm tall by 46 ± 2 nm across, corresponding to ~ 20 unit cells laterally and vertically.

The coverage and thickness of the films on the SLG surface was evaluated by scanning electron microscopy (SEM). A top-down micrograph of a COF-5 film grown on SLG/Cu for 30 min (Fig. 2E) indicates complete coverage of the film over the graphene surface. A few bulk COF-5 crystallites, observed in greater frequency when longer reaction times are used, are scattered on top of the film. They are not strongly associated to the underlying film, and most are removed by sonicating the substrate in dry toluene for 10 s, after which the micrographs are uniform over ~100-µm² areas. Grain boundaries in the COF film appear in the micrograph as thin dark lines that we attribute to the roughness of the underlying polycrystalline Cu layer, as they are not

Fig. 3. (A) Cross-sectional SEM image of a COF-5 film on SLG/Cu (30-min growth time, 195 ± 20-nm thickness) and (B) GID of the film. (C) Cross section of a COF-5 film on SLG/SiO₂ (2-hour growth time, 94 ± 5-nm thickness) and (D) GID of the film. (E) Cross section of a COF-5 film on SLG/SiC (8-hour growth time, 73 ± 3-nm thickness) and (F) GID of the film.



observed when COF-5 is grown on SLG on smoother substrates (for additional representative micrographs, see figs. S6 to S9). We obtained cross-sectional micrographs after depositing a protective layer of Pt (400 nm) and milling the sample with a Ga⁺ focused ion beam (FIB). The cross section of a film grown for 30 min (Fig. 3A) shows a continuous COF layer of 195 ± 20–nm thickness, corresponding to ~580 layers. The GID of this sample (Fig. 3B) was identical to that obtained from the 2-hour film (Fig. 2B), indicating similar crystallinity and alignment. A discontinuity in the Cu is illustrated in Fig. 3A; though the structure of the graphene at this defect is not known, the COF film conforms to the indentation.

Although these studies were performed on SLG supported by its Cu growth metal, our synthetic method is general for SLG transferred to other substrates, including transparent fused SiO2 (SLG/SiO₂). This flexibility facilitates studying the role of the underlying substrate on COF film growth and provides a direct route for incorporating COFs into a wide range of devices. COF-5 shows similar structure and alignment on SLG/SiO2 compared with SLG/Cu. The GID of a film (Fig. 3D, 2 hours reaction time) exhibits the same 100, 110, 200, 210, 220, 310, 400, 320, 330, 420, and 500 Bragg peaks with diffraction intensities all localized near $Q_{\perp} = 0$. A cross-sectional micrograph (Fig. 3C) of the film obtained after FIB milling shows a COF-5 film thickness of 94 \pm 5 nm, as well as a more uniform film/substrate interface compared with SLG/Cu. Top-down micrographs (fig. S10) show fewer bulk crystallites and none of the cracks observed in the films grown on SLG/Cu. Films grown on SLG/Cu are consistently thicker than those grown on SLG/SiO2 at equivalent reaction times (fig. S11), suggesting that the Cu surface (including its defect sites) plays a role in COF nucleation. Because the graphene on each substrate is derived from the same CVD process, we conclude that the thickness and uniformity of the film is strongly affected by the quality of the underlying substrate.

COF-5 films also form on SLG derived from the thermal decomposition of SiC from its Siterminated basal plane (SLG/SiC), SLG/SiC exhib-

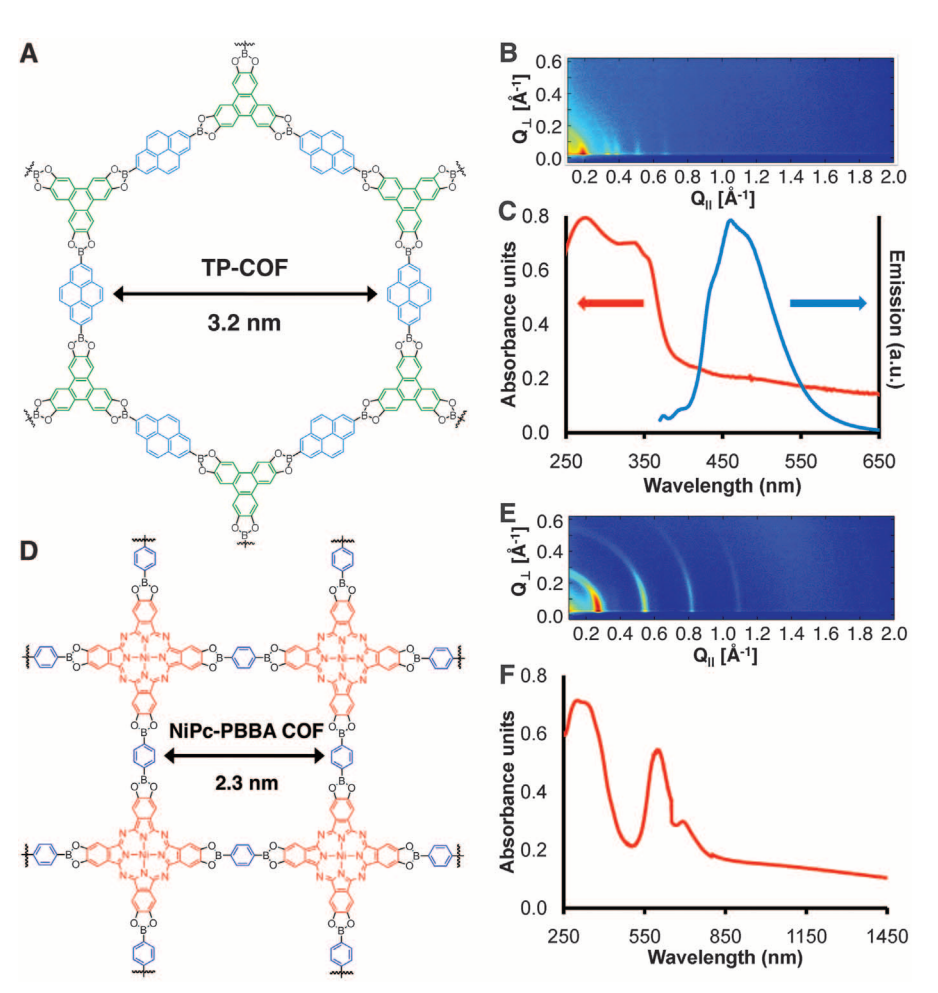


Fig. 4. (**A**) The TP-COF chemical structure, (**B**) GID of a film on SLG/SiO_2 , and (**C**) transmission UV/Vis spectrum and emission spectrum ($\lambda_{exc} = 352$ nm) of the film. a.u., arbitrary units. (**D**) The NiPc-PBBA COF chemical structure, (**E**) GID of a film on SLG/SiO_2 , and (**F**) transmission UV/Vis/NIR spectrum of the film.

its reduced surface roughness and larger graphene domains compared with SLG/Cu (26, 27). Topdown micrographs of COF-5 films grown for 8 hours indicate the formation of continuous films with no visible grain boundaries and few bulk crystallites (fig. S12). Cross-sectional micrographs obtained from FIB-milled samples indicate a uniform film with a thickness of 73 ± 3 nm (Fig. 3E and fig. S13). The relatively thin COF film

grown on SLG/SiC in 8 hours follows the thickness trend observed for SLG/Cu and SLG/SiO₂. GID of the film indicates similar diffraction patterns as those grown on the other substrates, suggesting a highly crystalline, vertically oriented film. The epitaxial relation between SLG and the single-crystal SiC substrate allowed us to determine that the COF-5 film does not grow epitaxially with respect to the graphene, as rotation of the sample

during the GID experiment did not reflect the sixfold symmetry of the COF lattice. This finding suggests that matching the COF lattice size and symmetry to the underlying graphene is not necessary to obtain crystalline films (see below).

The crystallinity and alignment of COF films on transparent SLG/SiO2 substrates provides a means to organize functional π -electron systems within optoelectronic devices. Accordingly, films of two of the first COF semiconductors were grown on SLG/SiO₂. One of these frameworks, known as triphenylene-pyrene (TP)-COF (11), arises from incorporating a pyrene-2,7-diboronic acid linker in place of PBBA into the hexagonal COF-5 lattice (Fig. 4A). We obtained TP-COF in both thin-film and powder form using similar conditions to those described above (see figs. S14 and S15 for powder characterization and figs. S16 and S17 for top-down and cross-sectional micrographs). The GID of the films (Fig. 4B) indicates similar vertical alignment of the 2D lattice, as judged by the attenuation of the signals with increasing Q_{\perp} and the absence of the out-ofplane 001 diffraction. The increased pore size of TP-COF is apparent from the prominent 100 diffraction at 0.19 Å^{-1} , and the $110 (0.34 \text{ Å}^{-1})$, 200 (0.39 Å^{-1}) , and 210 (0.52 Å^{-1}) are also observed. Refinement of these data provided lattice parameters a = b = 37.7 Å in excellent agreement with those derived from PXRD data of TP-COF powders (37.5 Å) (11). The transparent SLG/SiO₂ substrate enabled ultraviolet/visible/near infrared (UV/Vis/NIR) spectroscopy of a COF film in transmission mode for the first time (Fig. 4C, red trace). The spectrum is consistent with the presence of both HHTP and pyrene chromophores and shows improved vibrational resolution of the absorbance bands relative to the diffuse reflectance spectrum of the powder sample. The photoluminescence of the film (Fig. 4C, blue trace) is characteristic of pyrene excimer emission over all excitation wavelengths, arising from efficient energy transfer from HHTP to pyrene that was observed in TP-COF powders.

Finally, we confirmed that COFs lacking hexagonal symmetry may also be crystallized on SLG by preparing a Ni phthalocyanine-PBBA COF on SLG/SiO₂ (Fig. 4D). GID of the film (Fig. 4E) again exhibited diffraction peaks localized near $Q_{\perp} = 0$ located at 0.27 Å⁻¹ (100), 0.55 Å⁻¹ (200), 0.81 Å^{-1} (300), and 1.08 Å^{-1} (400). These data correspond to a vertically aligned 2D square lattice with parameters a = b = 23.0 Å that match those obtained from the characterization of the powder sample. Cross-sectional images indicate a continuous film of \sim 210 \pm 25–nm thickness (figs. S18 and S19). The translucent, turquoise films absorb strongly over the visible range of the spectrum as a consequence of the Ni phthalocyanine chromophores (Fig. 4F). Both the films and the powders are nonemissive, as is expected for H-aggregated phthalocyanines (see figs. S20 and S21 for powder characterization). These vertically aligned, porous phthalocyanine COFs are intriguing precursors of ordered heterojunction films long thought to be ideal for organic photovoltaic performance (28).

References and Notes

- 1. A. P. Côté et al., Science 310, 1166 (2005).
- A. P. Côté, H. M. El-Kaderi, H. Furukawa, J. R. Hunt,
 M. Yaghi, J. Am. Chem. Soc. 129, 12914 (2007).
- R. W. Tilford, W. R. Gemmill, H. C. zur Loye, J. J. Lavigne, Chem. Mater. 18, 5296 (2006).
- 4. D. F. Perepichka, F. Rosei, Science 323, 216 (2009).
- 5. H. M. El-Kaderi et al., Science 316, 268 (2007).
- 6. L. Grill et al., Nat. Nanotechnol. 2, 687 (2007).
- N. A. A. Zwaneveld et al., J. Am. Chem. Soc. 130, 6678 (2008).
- 8. A. Gourdon, Angew. Chem. Int. Ed. 47, 6950 (2008).
- M. In't Veld, P. lavicoli, S. Haq, D. B. Amabilino, R. Raval, Chem. Commun. 2008 1536 (2008).
- S. Wan, J. Guo, J. Kim, H. Ihee, D. Jiang, Angew. Chem. Int. Ed. 48, 5439 (2009).
- S. Wan, J. Guo, J. Kim, H. Ihee, D. Jiang, Angew. Chem. Int. Ed. 47, 8826 (2008).
- 12. E. L. Spitler, W. R. Dichtel, *Nat. Chem.* **2**, 672 (2010).
- 13. X. Ding et al., Angew. Chem. Int. Ed. 50, 1289 (2011).

- 14. X. Li et al., Nano Lett. 9, 4359 (2009).
- 15. A. Kumar, C. Zhou, ACS Nano 4, 11 (2010).
- 16. A. Reina et al., Nano Lett. 9, 30 (2009).
- 17. K. S. Kim et al., Nature 457, 706 (2009).
- 18. X. Li et al., Science **324**, 1312 (2009); 10.1126/
- M. P. Levendorf, C. S. Ruiz-Vargas, S. Garg, J. Park, *Nano Lett.* 9, 4479 (2009).
- 20. S. Bae et al., Nat. Nanotechnol. 5, 574 (2010).
- 21. Materials and methods are available as supporting material on *Science* Online.
- D. M. Smilgies, D. R. Blasini, J. Appl. Cryst. 40, 716 (2007).
- 23. B. Lukose, A. Kuc, T. Heine, Chemistry 17, 2388 (2011).
- 24. J. L. Baker et al., Langmuir 26, 9146 (2010).
- 25. D. M. Smilgies, J. Appl. Cryst. 42, 1030 (2009).
- 26. C. Berger *et al.*, *Science* **312**, 1191 (2006); 10.1126/ science.1125925.
- 27. K. V. Emtsev et al., Nat. Mater. 8, 203 (2009).
- A. C. Mayer, S. R. Scully, B. E. Hardin, M. W. Rowell,
 M. D. McGehee, *Mater. Today* 10, 28 (2007).

Acknowledgments: This research was supported by startup funds provided by Cornell University and the NSF-funded CCI-I Center for Molecular Interfacing (CHE-0847926). This work is based on research conducted at the Cornell High Energy Synchrotron Source (CHESS), which is supported by the NSF and the NIH/National Institute of General Medical Sciences under NSF award DMR-0936384. We also made use of the Cornell Center for Materials Research facilities with support from the NSF Materials Research Science and Engineering Centers program (DMR-0520404). J.W.C. thanks the NSF for the award of a Graduate Research Fellowship; E.L.S. thanks the NSF for the award of the American Competitiveness in Chemistry postdoctoral fellowship (CHE-0936988); and M.G.S. (FA9550-07-1-0332) and J.P. (FA9550-09-1-0691) thank the Air Force Office of Scientific Research. We thank D. Smilgies for helpful discussions and K. Cox for technical illustration assistance. A provisional patent application based on this work has been filed by Cornell University (USA 61/382,093).

Supporting Online Material

www.sciencemag.org/cgi/content/full/332/6026/228/DC1 Materials and Methods SOM Text

Figs. S1 to S21

csuttle@eos.ubc.ca

11 January 2011; accepted 28 February 2011 10.1126/science.1202747

A Virophage at the Origin of Large DNA Transposons

Matthias G. Fischer¹ and Curtis A. Suttle^{1,2,3}*

DNA transposons are mobile genetic elements that have shaped the genomes of eukaryotes for millions of years, yet their origins remain obscure. We discovered a virophage that, on the basis of genetic homology, likely represents an evolutionary link between double-stranded DNA viruses and *Maverick/Polinton* eukaryotic DNA transposons. The Mavirus virophage parasitizes the giant *Cafeteria roenbergensis* virus and encodes 20 predicted proteins, including a retroviral integrase and a protein-primed DNA polymerase B. On the basis of our data, we conclude that *Maverick/Polinton* transposons may have originated from ancient relatives of Mavirus, and thereby influenced the evolution of eukaryotic genomes, although we cannot rule out alternative evolutionary scenarios.

Transposable elements (TEs) affect the genetic landscape of eukaryotes by creating new alleles, influencing gene regulation, and rearranging chromosome structure (1). TEs

can be divided into retrotransposons and DNA transposons. DNA transposons are further categorized into cut-and-paste TEs, rolling-circle TEs, and the self-synthesizing *Maverick* or *Polinton*

(MP) TEs (2). MP TEs are 9 to 22 kilobase pairs (kb) long, encode up to 20 proteins, and are found in a wide range of eukaryotes, including protists, fungi, and animals (3–6). Their coding capacity varies among species, yet they contain a conserved set of genes (4, 5). Most MP TEs encode a retroviral integrase, a viral protein-primed DNA polymerase B, an adenosine triphosphatase (ATPase) similar to the FtsK-HerA genome-packaging ATPases of double-stranded DNA (dsDNA) viruses, and a cysteine protease with homologs in adenoviruses. Another protein termed

¹Department of Microbiology and Immunology, 1365–2350 Health Sciences Mall, University of British Columbia, Vancouver V6T 1Z3, Canada. ²Department of Botany, 3529–6270 University Boulevard, University of British Columbia, Vancouver V6T 1Z4, Canada. ³Department of Earth and Ocean Sciences, 6339 Stores Road, University of British Columbia, Vancouver V6T 1Z4, Canada.

*To whom correspondence should be addressed. E-mail: